Quantification of Serotonin 5-HT$_{1A}$ Receptors in Monkey Brain With [^{11}C](R)-(−)-RWAY

FUMIHIKO YASUNO,[1]* **SAMI S. ZOGHBI,**[1] **JULIE A. McCARRON,**[1] **JINSOO HONG,**[1]
MASANORI ICHISE,[1] **AMIRA K. BROWN,**[1] **ROBERT L. GLADDING,**[1] **JOHN D. BACHER,**[2]
VICTOR W. PIKE,[1] AND **ROBERT B. INNIS**[1]
[1]*Molecular Imaging Branch, National Institute of Mental Health, Bethesda, Maryland*
[2]*Division of Veterinary Resources, Office of Research Services, National Institutes of Health, Bethesda, Maryland*

KEY WORDS　　serotonin 5-HT$_{1A}$; [^{11}C](R)-(−)-RWAY; kinetic analysis; P-glycoprotein; PET

ABSTRACT　　[^{11}C](R)-(−)-RWAY ([^{11}C]2, 3, 4, 5, 6, 7-hexahydro-1{4-[1[4-(2-methoxy-phenyl)-piperazinyl]]-2-phenylbutyry}-1H-azepine) is a new radioligand for imaging brain 5-HT$_{1A}$ receptors with positron emission tomography. In [^{11}C](R)-(−)-RWAY, the direction of the amide bond is expected to reduce metabolism by hydrolysis while allowing easy ^{11}C-labeling at the methoxy position. The purposes of this study were to evaluate different tracer kinetic models in nonhuman primates to quantify 5-HT$_{1A}$ receptors with [^{11}C](R)-(−)-RWAY and to test for the possible action of P-glycoprotein (P-gp), one of the known efflux pumps at the blood–brain barrier. The brain uptake of radioactivity from [^{11}C](R)-(−)-RWAY into 5-HT$_{1A}$ receptor-rich brain regions was severalfold greater than for its antipode ([^{11}C](S)-(+)-RWAY) and could be displaced by receptor saturating doses of the selective 5-HT$_{1A}$ antagonist, WAY-100635. Pretreatment with tariquidar, a potent inhibitor of P-gp, increased brain uptake of [^{11}C](R)-(−)-RWAY about 1.5-fold and the plasma free fraction about 1.8-fold. Thus, the effect of tariquidar on brain uptake may have been caused by displacement of the radioligand binding to plasma proteins. Mathematical modeling showed that the estimated values of regional binding potential were correlated strongly between two-tissue compartment model and multilinear reference tissue model, and thus, supported the use of the cerebellum as a reference region. **Synapse 60:510–520, 2006.** Published 2006 Wiley-Liss, Inc.[†]

INTRODUCTION

The first successful positron emission tomography (PET) radioligand for the human 5-HT$_{1A}$ receptor was WAY-100635 labeled with ^{11}C in the *O*-methoxy position (Pike et al., 1995) (Fig. 1A). Unfortunately, [*O*-methyl-^{11}C]WAY-100635 is rapidly metabolized in human and nonhuman primates with cleavage of the amide bond. The resulting radiometabolite, [*O*-methyl-^{11}C]WAY-100634, enters brain in a significant (Osman et al., 1998). Because of this metabolic path, WAY-100635 was labeled in the carbonyl position (McCarron et al., 1996), since amide cleavage of [carbonyl-^{11}C] WAY-100635 generates the polar metabolite, [carboxyl-^{11}C]cyclohexanecarboxylic acid, that does not easily cross the blood–brain barrier (Pike et al., 1996) (Fig. 1B).

Two disadvantages of [carbonyl-^{11}C]WAY-100635 are: (1) labeling in the carbonyl position is more difficult than >O-methylation and (2) nonspecific uptake in cere-

bellum is low. Reference tissue analysis is strongly preferred to standard compartmental modeling, because it does not require arterial line placement or radiometabolite analysis. This relatively simple method calculates the ratio of brain uptake in receptor-rich to receptor-free regions, and assumes that all activity derives from the parent tracer and not radiometabolite(s). In the case of [carbonyl-^{11}C]WAY-100635, the denominator (cerebellar activity) is so low that the ratio is vulnerable to measurement error and to even small amounts of radiometabolite(s). We developed [*O*-methyl-^{11}C](R)-(−)-RWAY
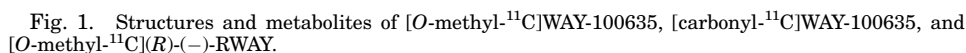
Fig. 1. Structures and metabolites of [*O*-methyl-^{11}C]WAY-100635, [carbonyl-^{11}C]WAY-100635, and [*O*-methyl-^{11}C](*R*)-(−)-RWAY.

(denoted here as [^{11}C](*R*)-(−)-RWAY) to correct these two deficiencies of [carbonyl-^{11}C]WAY-100635 (Fig. 1C). Specifically, the amide bond was reversed with the goal of slowing metabolism of the tracer and washout from brain (McCarron et al., 2004; Shetty et al., 2005). In addition, the compound was labeled in the relatively easy *O*-methyl position. The specificity and affinity of (*R*)-(−)-RWAY were measured with human receptors in transfected cell lines by the NIMH-funded Psychopharmacology Drug Screening Program. The K_i values of this compound were: 0.6 nM at 5-HT$_{1A}$, 7.2 nM at 5-HT$_{2B}$, 9.5 nM at 5-HT$_{1D}$, and greater than 65 nM for the remaining 5-HT subtypes.

The primary purpose of this study was to carefully examine the kinetics of [^{11}C](*R*)-(−)-RWAY in nonhuman primates and to determine whether human studies would be justified. Specifically, we have assessed the pharmacological specificity of brain uptake and compared arterial input compartmental methods with reference tissue analysis. A secondary aim of this study was to examine the effect, if any, of brain efflux pumps such as P-glycoprotein (P-gp) on the measurement of distribution volume. The human genome contains 48 genes that encode these ATP binding cassette transporters (Aloyo et al., 1993; Ambudkar et al., 2003). At least one of them (P-gp) and probably others reside at the blood–brain barrier and remove lipophilic drugs while in transit through the membrane (Vaalburg et al., 2005). These efflux pumps not only reduce activity in brain but may also confound quantification of receptor binding. Furthermore, some concomitant medications (such as fexofenadine or Allegra®) are not only substrates but can block the efflux of other drugs (Elsinga et al., 2004). Previous studies have suggested that WAY-100635 and some of its analogs (e.g., MPPF) are substrates for P-gp (Passchier et al., 2000). We used the potent and selective P-gp inhibitor tariquidar (XR9576) (Roe et al., 1999) to determine if [^{11}C](*R*)-(−)-RWAY is also a substrate for this efflux pump in non-human primates.

MATERIALS AND METHODS
Animals

We used eight male rhesus monkeys (weight: 12.1 ± 2.6 kg, with these and subsequent data expressed as mean ± SD), four of which underwent arterial blood sampling. Animals were immobilized with ketamine (10 mg/kg i.m.) to allow intubation. After transportation to the PET suite, the animals were placed under isoflurane anesthesia (1–2%), and the head was immobilized in a stereotactic frame. To minimize the effects of ketamine, scans started at least 90 min after ketamine administration.

We used two PET cameras: the GE Advance device (General Electric Medical Systems, Waukesha, WI) was used for analysis of the comparison of enantiomers, the preblockade with other WAY100635, and the quantification analysis and the High Resolution Research Tomograph (HRRT; Siemens/CPS, Knoxville, TN) device for the effect of P-gp blockade with tariquidar. The Advance and HRRT differ in performance characteristics. The reconstructed resolution is 6 mm full-width half-maximum and 2.5 mm full-width half-maximum in all directions in 3D mode. The difference in performance did not affect our comparison, since the studies examined separate parameters e.g., different scanner was used for different study. Nevertheless, Tables II–IV use data only from the GE Advance, and Table V from the HRRT.

TABLE I. PET studies performed with $[^{11}C](R)$-(–)-RWAY

Study	Scanner	Scan duration (min)	Condition
1	Advance	90	(–)-and (+)-RWAY
2	Advance	90	Baseline and preblocking with WAY100635
3	Advance	90	Baseline
4	Advance	90	Baseline
5	Advance	120	Baseline
6	HRRT	90	Baseline and pretreatment with tariquidar
7	HRRT	120	Baseline and pretreatment with tariquidar
8	HRRT	120	Baseline and pretreatment with tariquidar

$[^{11}C]$ (R)-(–)-$[^{11}C]$RWAY was prepared as described previously (McCarron et al., 2004). $[^{11}C](R)$-(–)-RWAY was administered over ~60 s, with injected activity of 220 ± 45 MBq and specific activity of 41 ± 13 GBq/mmol. Scans of 90 min (27 frames) were acquired in five studies (Table I, Studies 1–4 and 6), whereas longer scans (33 frames over 120 min) were acquired in three studies (Table I, Studies 5, 7, and 8).

Arterial blood was collected in heparin-treated syringes from three monkeys at 30, 45, and 60 s and 3, 5, 10, 30, 60, and 90 min after injection (Table I, Studies 2–4), and from one monkey at 30, 45, 60, 75, 90, 105, and 120 s and 3, 5, 10, 30, 60, and 90 min after injection (Table I, Study 5). The parent tracer, separated from radiometabolites, was measured as previously described (Zoghbi et al., 2005).

One monkey was used to compare brain uptake of the more effective ($[^{11}C](R)$-(–)-RWAY) and the less effective ($[^{11}C](S)$-(+)-RWAY) enantiomer (Table I, Study 1). Another monkey was used for a receptor blocking study, in which nonradioactive WAY-100635 (0.5 mg/kg i.v.) was injected 15 min before $[^{11}C](R)$-(–)-RWAY (Table I, Study 2). We compared the uptake of $[^{11}C](R)$-(–)-RWAY in three monkeys with and without the administration of tariquidar (8 mg/kg i.v.) (Table I, Studies 6–8).

Each monkey had a T1-weighted magnetic resonance imaging (MRI) scan on a GE Signa 1.5 T scanner (SPGR, TR/TE/flip angle = 13.1 ms/5.8 ms/45°, $0.4 \times 0.4 \times 1.5$ mm^3 with coronal acquisitions on a $256 \times 256 \times 60$ matrix).

Image analysis

PET and MR images were coregistered with SPM2 (Wellcome Department of Cognitive Neurology, London, UK). Five regions of interest (ROIs) were manually defined on summed coronal PET images from 30 min to the end of study, with reference to the animal's coregistered MRI and a brain MRI atlas (Paxinos et al., 2000). The five ROIs were: cerebellum, prefrontal cortex, lateral temporal cortex, medial temporal region including the hippocampus, and dorsal raphe, with region of interest (ROI) size ranging from 112 to 8256 mm^3.

Estimation of distribution volume with arterial input function

ROI time–activity data were analyzed with both one-tissue and two-tissue compartment models (1-TCM and 2-TCM) (Cunningham and Lammertsma, 1995) using the metabolite-corrected plasma input function. Rate constants were estimated with weighted least squares and the Marquardt optimizer. Binding potential (BP) was calculated as k_3/k_4 in 2-TCM and called the "direct BP."

To compare BP estimates with the reference tissue model further estimates were obtained as follows:

$$\text{Indirect BP } = (V_T \text{ region}/V_T \text{ cerebellum}) - 1 \qquad (1)$$

where V_T is the total distribution volume. With 1-TCM, $V_T = K_1/k_2$; with 2-TCM, $V_T = K_1/k_2(1 + k_3/k_4)$. The equation assumes that the distribution volume of free and nonspecifically bound ligand is the same in target and reference regions of brain (Gunn et al., 1998).

Time-stability of parameter estimates

The relationship between parameter estimates and the duration of the scan was analyzed in one monkey with increasingly truncated data sets from 0–120 to 0–40 min (Table I, Study 5). The estimated parameters were compared with the reference values obtained with the complete 120-min data set. For cerebellum and all target regions, V_T and indirect BP were estimated in the 2-TCM. The solution was considered stable after time t if the result was within 5% of that from the analysis of the entire data set (i.e., 0–120 min).

Estimation of distribution volume ratio without arterial blood sampling

To estimate distribution volume ratio without arterial blood sampling, the data were analyzed in five monkeys (Table I, Studies 1–5) with simplified reference tissue model (SRTM) (Lammertsma and Hume, 1996) and two versions of a multilinear reference tissue model (MRTM and MRTM2) (Ichise et al., 2003). Two-parameter MRTM2 was considered to be more resistant to noise than three-parameter MRTM. MRTM2 requires a priori estimation of k_2 of cerebellum (k'_2), which can be estimated by MRTM (Ichise et al., 2003). The value of k'_2 was the mean weighted (according to ROI size) value from prefrontal cortex, temporal cortex, dorsal raphe, and medial temporal region. Initially, start time t^* was determined from graphical analysis (Logan et al., 1990) and set at 30 min. The accuracy of this start time was later
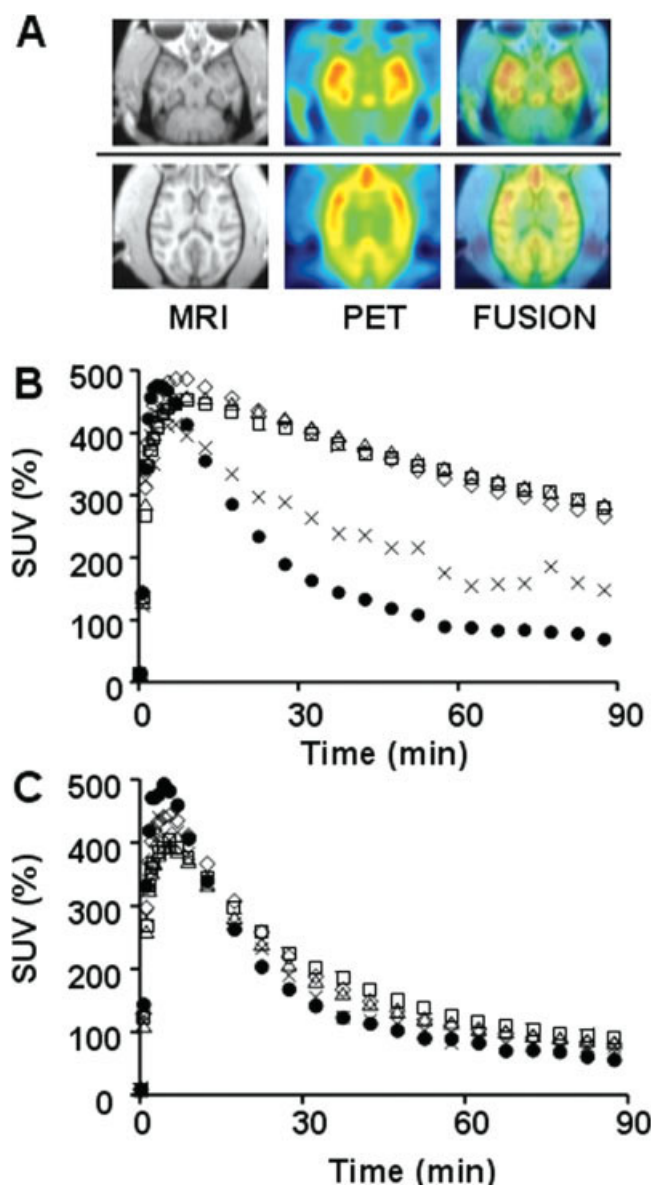
Fig. 2. Uptake of [^{11}C](R)-(−)-RWAY in rhesus brain. (**A**) PET images (middle) of [^{11}C](R)-(−)-RWAY were summed from 30 to 90 min. The corresponding MR images are on left, and the fused PET and MR images are on right. (**B**) and (**C**) Time course of regional brain activities after injection of (B) [^{11}C](R)-(−)-RWAY and (C) [^{11}C](S)-(+)-RWAY. Activity is shown as % SUV (standard uptake value) which normalizes for injected dose and body weight. % SUV = (% injected activity/cm^3 tissue) × (gram body weight). Cerebellum (●), prefrontal cortex (△), lateral temporal cortex (◇), dorsal raphe (□), and medial temporal region (×).

examined by comparing the estimates with that of 2-TCM (see Results). The kinetic and reference tissue analyses were performed using the software program PMOD 2.65 (Burger et al., 1998).

Effect of P-gp on brain uptake and peripheral disposition of [^{11}C](R)-(−)-RWAY

We compared the uptake of [^{11}C](R)-(−)-RWAY in three monkeys (Table I, Studies 6–8) with and without
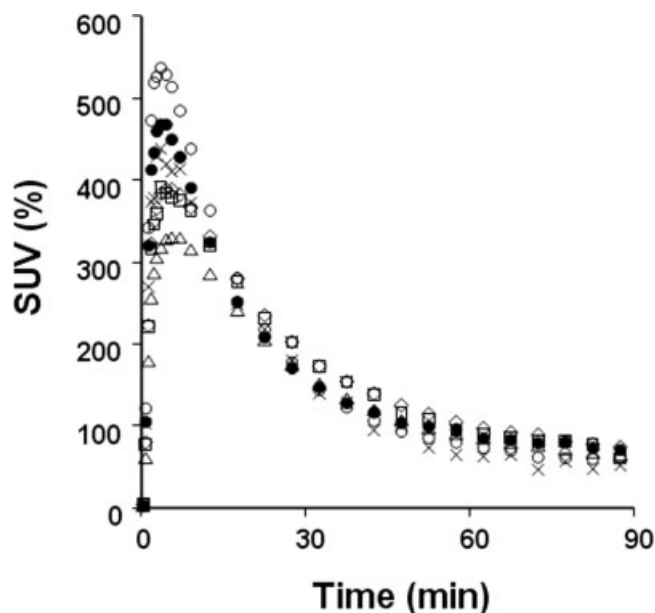
Fig. 3. Brain uptake of [^{11}C](R)-(−)-RWAY blocked by pretreatment with WAY-100635 (0.5 mg/kg i.v.) before injection of [^{11}C](R)-(−)-RWAY. Regional brain uptake in the preblocked condition (●, △, ◇, □, ×) was similar to the baseline cerebellar uptake (○). Cerebellum (●, ○), prefrontal cortex (△), lateral temporal cortex (◇), dorsal raphe (□), and medial temporal region (×).

the administration of the P-gp inhibitor tariquidar (8 mg/kg i.v.) 30 min before the radioligand. The scans with tariquidar were acquired 1 h after the end of the first baseline scans.

We measured and compared the plasma free fraction (f_1) in addition to the uptake of [^{11}C](R)-(−)-RWAY with and without administration of tariquidar. Plasma free fraction was measured by ultrafiltration through Centrifree membrane filters (Amicon Division, W.R. Grace and Co., Danvers, MA) (Gandelman et al., 1994).

Statistical analysis

Goodness-of-fit by nonlinear least squares analysis was evaluated using the model selection criterion (MSC), which is a modification of the Akaike information criterion (AIC) (Akaike, 1974). MSC gives greater values for better fitting. Goodness-of-fit by 1-TCM and 2-TCM was compared with F statistics (Hawkins et al., 1986).

The standard errors of nonlinear least squares estimation for rate constants were given by the diagonal of the covariance matrix (Carson, 1986) and expressed as a percentage of the rate constants (coefficient of variation, % COV). In addition, % COV of total distribution volume was calculated from the covariance matrix using the generalized form of error propagation equation (Bevington and Robinson, 2003), where correlations among parameters were taken into account.
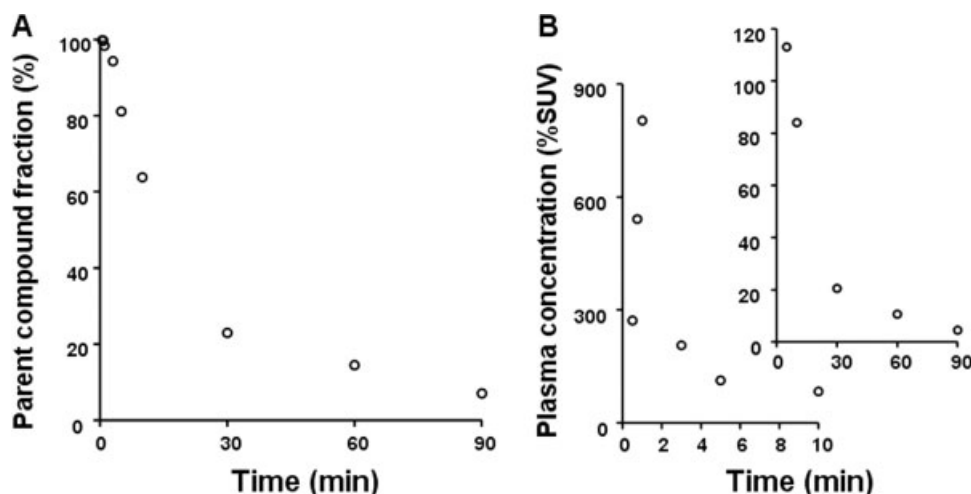
Fig. 4. (**A**) Mean percentage ratio of unchanged [^{11}C](−)-RWAY in plasma ($n = 4$). (**B**) Mean [^{11}C](−)-RWAY plasma concentration, corrected for metabolites, during 90 min interval after radioligand injection. Because of the large range of plasma concentrations during the study, the curve is shown with two time intervals: 0–10 and 5–90 min, with two points (5 and 10 min) plotted on both curves.

TABLE II. Parameter estimates (mean ± SD) obtained from a two-tissue compartment model

Region	K_1 (% COV)	k_2 (% COV)	k_3 (% COV)	k_4 (% COV)	Direct BP (% COV)	V_T (% COV)	Indirect BP	MSC
Cerebellum	0.48 ± 0.15	0.14 ± 0.04	0.03 ± 0.02	0.04 ± 0.02	0.86 ± 0.1	6.47 ± 1.06	–	5.3 ± 1.0
	1.6 ± 0.5	4.4 ± 1.7	18.5 ± 2.8	14.0 ± 6.2	8.2 ± 1.8	2.6 ± 1.4		
Prefrontal cortex	0.24 ± 0.02	0.08 ± 0.02	0.15 ± 0.08	0.03 ± 0.01	5.21 ± 0.8	18.1 ± 1.7	1.84 ± 0.44	5.8 ± 1.0
	1.4 ± 0.5	4.4 ± 1.7	11.7 ± 2.6	8.1 ± 4.1	10.3 ± 2.7	2.2 ± 1.3		
Lateral temporal cortex	0.27 ± 0.03	0.08 ± 0.02	0.15 ± 0.08	0.03 ± 0.01	4.91 ± 0.39	18.3 ± 2.3	1.86 ± 0.30	5.6 ± 1.3
	1.7 ± 0.9	10.0 ± 1.5	12.2 ± 2.2	7.7 ± 3.3	9.5 ± 0.7	2.3 ± 1.6		
Dorsal raphe region	0.32 ± 0.08	0.39 ± 0.59	0.33 ± 0.49	0.03 ± 0.01	16.1 ± 19.5	12.7 ± 3.1	0.95 ± 0.23	3.6 ± 1.2
	9.4 ± 8.7	26.7 ± 22.0	17.7 ± 8.9	15.0 ± 8.4	19.8 ± 13.3	3.2 ± 1.5		
Medial temporal region	0.28 ± 0.04	0.11 ± 0.03	0.19 ± 0.11	0.03 ± 0.01	7.21 ± 3.14	20.2 ± 2.9	2.15 ± 0.38	5.2 ± 1.2
	2.3 ± 1.1	13.8 ± 6.7	13.8 ± 5.2	9.9 ± 6.2	12.6 ± 6.1	2.7 ± 1.6		

BP, binding potential; V_T, total distribution volume; MSC, model selection criteria; direct BP = k_3/k_4; indirect BP = (V_T region/V_T cerebellum) − 1.

TABLE III. Parameter estimates (mean ± SD) obtained from a one-tissue compartment model

Region	K_1 (% COV)	k_2 (% COV)	V_T (% COV)	Indirect BP	MSC
Cerebellum	0.41 ± 0.13	0.08 ± 0.03	5.4 ± 1.0	–	2.9 ± 0.5
	3.4 ± 1.0	6.0 ± 1.8	3.8 ± 1.4		
Prefrontal cortex	0.19 ± 0.02	0.01 ± 0.003	14.9 ± 3.2	1.78 ± 0.40	2.8 ± 0.9
	2.4 ± 1.2	5.5 ± 2.2	3.8 ± 1.4		
Lateral temporal cortex	0.22 ± 0.01	0.02 ± 0.004	15.0 ± 3.3	1.80 ± 0.42	2.5 ± 1.0
	2.6 ± 1.4	5.7 ± 2.3	4.0 ± 1.4		
Dorsal raphe region	0.22 ± 0.02	0.02 ± 0.005	11.0 ± 2.6	1.06 ± 0.37	2.0 ± 0.7
	3.1 ± 1.1	6.0 ± 1.8	4.1 ± 1.1		
Medial temporal region	0.22 ± 0.01	0.01 ± 0.004	16.7 ± 4.0	2.11 ± 0.55	2.5 ± 1.1
	2.7 ± 1.5	6.1 ± 2.4	4.3 ± 1.5		

BP, binding potential; V_T, total distribution volume; MSC, model selection criteria; indirect BP = (V_T region/V_T cerebellum) − 1.

RESULTS
Brain uptake of [^{11}C](R)-(−)-RWAY and [^{11}C](S)-(+)-RWAY

For the more active enantiomer [^{11}C](R)-(−)-RWAY, brain uptake was highest in medial and lateral temporal region, prefrontal cortex, and dorsal raphe region and low in cerebellum (Figs. 2A and 2B). In contrast, the uptake of the less effective enantiomer, [^{11}C](S)-(+)-RWAY, in all brain regions was similar to that of the more effective enantiomer in cerebellum (Figs. 2B and 2C). The brain uptake of [^{11}C](R)-(−)-RWAY was blocked with receptor saturating doses of WAY-100635 (0.5 mg/kg i.v.; Fig. 3).

Arterial plasma analysis

The radioligand was quickly metabolized and represented (81 ± 3)%, (29 ± 8)%, and (15 ± 3)% of total plasma activity at 5, 20, and 60 min, respectively (Fig. 4A). Plasma activity of unchanged [^{11}C](R)-(−)-RWAY peaked at ∼1 min and decreased to (4 ± 3)% of the peak by 20 min (Fig. 4B).

Nonlinear least squares compartmental analyses

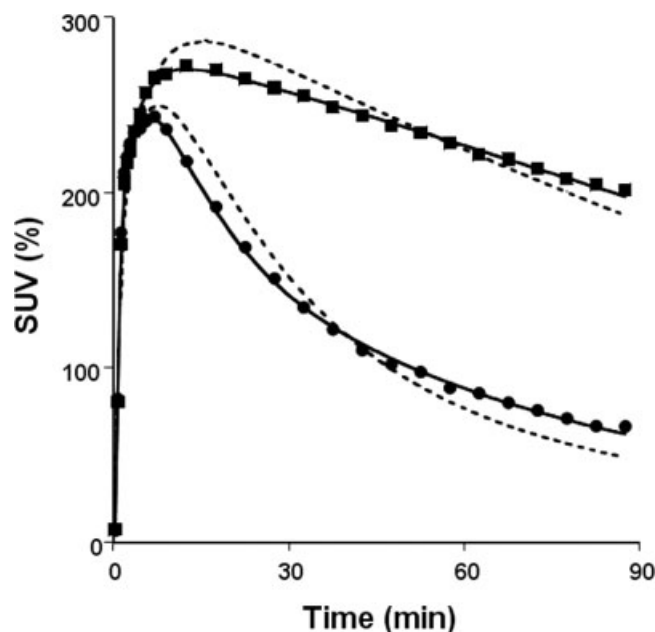Convergence was achieved in all regions and all animals ($n = 4$) with both 1-TCM and 2-TCM analyses

Fig. 5. One-and two-tissue compartment analysis. Fitting by 2-TCM (solid line) was significantly better that that by 1-TCM (dashed line) for both cerebellum (●) and lateral temporal cortex (■).
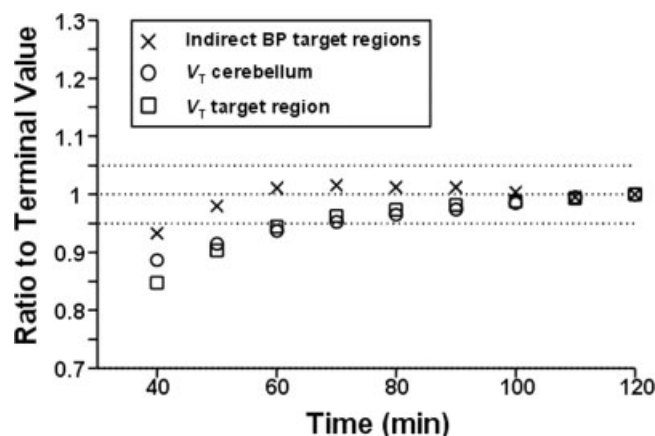

Fig. 6. Time stability of parameter estimation. Relationship between the parameter estimates obtained by 2-TCM and the experiment duration in all target regions (prefrontal cortex, lateral temporal cortex, dorsal raphe, and medial temporal region) as well as cerebellum. Each point represents the estimated value from one monkey, analyzed with data from 0 to the specified time, and expressed as a percentage of the 120-min value.

with 90-min scan data, but the 2-TCM provided significantly better fit to the measured data (Tables II and III; Fig. 5). MSC (Model Selection Criteria) values were higher for 2-TCM (5.10 ± 0.88) than for 1-TCM fits (2.55 ± 0.34), and this difference was significant by F-test in all regions of all animals ($P < 0.001$).

In 2-TCM, the standard errors of individual rate constants k_2, k_3, and k_4 (but not K_1) as well as direct BP values showed poor identifiability with COV values > 10% in most regions. However, V_T was relatively

TABLE IV. BP values obtained from reference tissue models

Region	BP (mean ± SD)		
	SRTM	MRTM	MRTM2
Prefrontal cortex	1.45 ± 0.47	1.55 ± 0.44	1.57 ± 0.43
Lateral temporal cortex	1.47 ± 0.32	1.58 ± 0.28	1.57 ± 0.27
Dorsal raphe region	0.77 ± 0.14	0.87 ± 0.25	0.81 ± 0.21
Medial temporal region	1.68 ± 0.32	1.74 ± 0.31	1.79 ± 0.30

BP, binding potential; SRTM, simplified reference tissue model; MRTM and MRTM2, three parameter and two parameter multilinear reference tissue model.
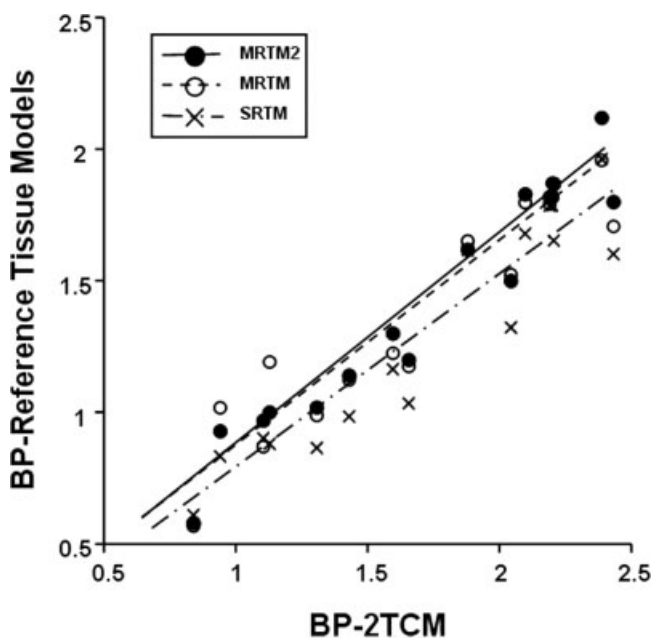
Fig. 7. Correlation of BP estimated from reference tissue (MRTM, MRTM2, and SRTM) and plasma-input two-tissue compartmental methods ($n = 4$). The correlation coefficient was higher with MRTM2 ($r = 0.97$) than with MRTM ($r = 0.93$) and SRTM ($r = 0.93$). The slope of the correlation line indicated that BP values from MRTM2 were 18% lower than those from 2-TCM, although its degree of underestimation was smaller than that of SRTM (25%). The equation of the line with y-intercept set to 0 is: $y = 0.82x$ (MRTM2); $y = 0.81x$ (MRTM); $y = 0.75x$ (SRTM).

well identified in each model, with COV values < 4%. Although V_T values obtained by these two models correlated well ($r = 0.96$) and they provided similar indirect BP values for each region, 1-TCM apparently underestimated V_T by an average of 17% (range, 5–30%), which may have been caused by its poor goodness of fit.

Time stability of parameter estimates

The time stability of parameter estimation was analyzed for the cerebellum and four receptor-rich regions (prefrontal cortex, lateral temporal cortex, dorsal raphe, and medial temporal region), with the latter reported as the volume-weighted mean of the four target regions. We defined significant bias with the relatively strict criterion of > ±5% of the value determined
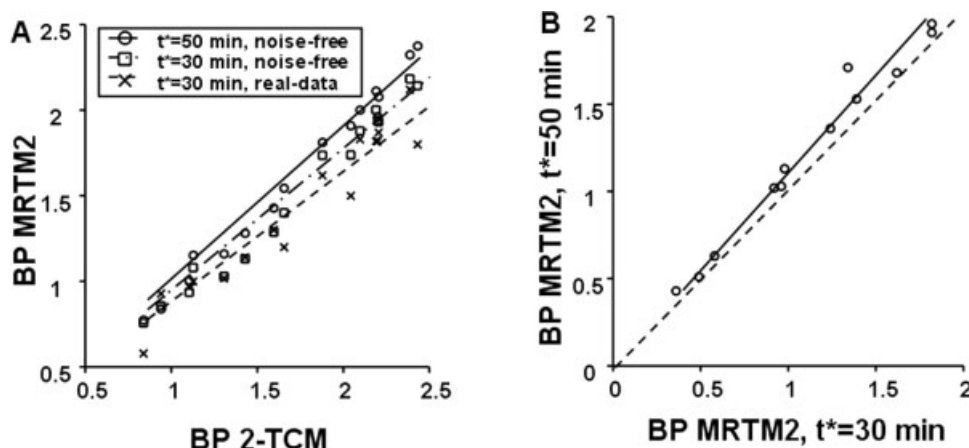
Fig. 8. Effect of noise, start time, and scan duration on BP calculated with MRTM2. (**A**) BP values from MRTM2 were 18% lower than those from 2-TCM, but this underestimation was reduced to 12% with noise-free data. Increasing t^* from 30 to 50 min further reduced the underestimation to 6%. The equations of the lines with y-intercept set to 0 are: $y = 0.82x$, $r = 0.94$ ($t^* = 30$ min, real data);

$y = 0.88x$, $r = 0.99$ ($t^* = 30$ min, noise-free data); and $y = 0.94x$, $r = 0.99$ ($t^* = 50$ min, noise-free data). (**B**) Increasing the scan duration from 90 to 120 min and the start time from 30 to 50 min, respectively, caused a 10% increase of BP calculated with MRTM2. The equation of the solid line with y-intercept set to 0 is: $y = 1.10x$, $r = 0.99$. The dashed line of unity shows $y = x$.
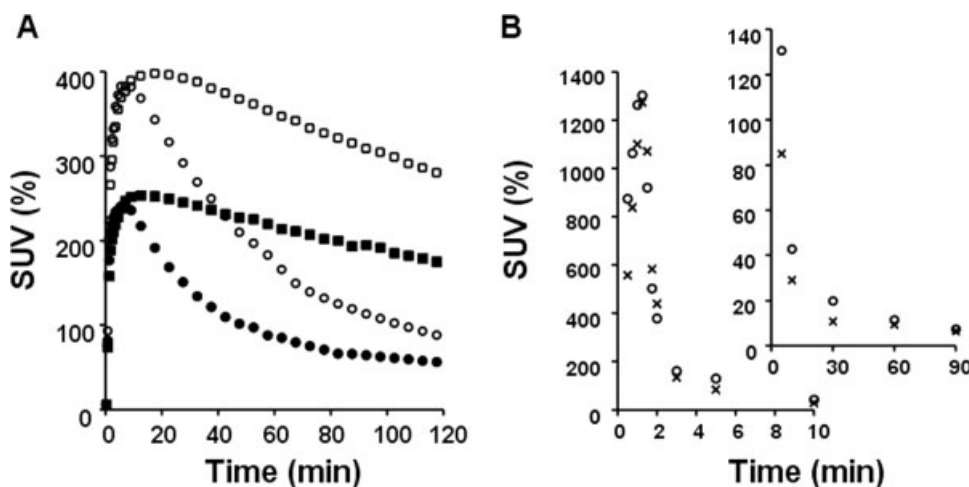
Fig. 9. Effect of tariquidar on brain uptake and peripheral clearance of [^{11}C](R)-(−)-RWAY. (**A**) Tariquidar (8 mg/kg i.v. 30 min before radiotracer) markedly increased the uptake in both target (square) and background (circle) regions. Solid symbols (■, ●) are used for baseline and open symbols (□, ○) for tariquidar results. The target region is the volume-weighted average of prefrontal cortex, lateral temporal cortex, dorsal raphe, and medial temporal region. (**B**) [^{11}C](R)-(−)-RWAY plasma radioactivity, corrected for

metabolites, are shown for baseline (○) and tariquidar (×) studies. Because of the large range of plasma concentrations during the study, the curve is shown with two time intervals: 0–10 and 5–90 min, with two points (5 and 10 min) plotted on both curves. The curves suggest no significant effect of tariquidar on peripheral clearance. In fact, the AUC of the plasma curves determined from the trapezoidal integration method actually showed a 12% decrease with tariquidar.

with the entire 120-min data set. For 2-TCM, no significant bias was found for V_T in any target region or cerebellum for the durations > 70 min. Indirect BP showed no significant bias for the durations > 50 min and was remarkably stable for durations > 60 min (Fig. 6).

Linearized reference tissue analysis

With the scan durations of 90 min and $t^* > 40$ min, MRTM did not converge in small areas such as raphe and medial temporal region in two of five monkeys.

The effect of noise was larger with $t^* > 40$ min, since we could not get adequate number of points for linear regression with this late start time and the scan duration (Ichise et al., 2002). We applied t^* of 30 min with scans of 90-min duration. MRTM and MRTM2 provided similar BP values for each region, but BP values derived from SRTM was smaller than those from MRTM and MRTM2 (Table IV). In addition, BP values of reference tissue methods were well correlated with those obtained using 2-TCM (indirectly derived from V_T) ($n = 4$), but the correlation coefficient was higher

TABLE V. Brain area under the curve (AUC) and plasma free fraction (f_1): Baseline and tariquidar administration

Study	f_1 Baseline	f_1 Tariquidar	Ratio (tariquidar/baseline) F_1	Ratio (tariquidar/baseline) AUC cerebellum	Ratio (tariquidar/baseline) AUC target
6	2.33	4.70	2.02	1.25	1.36
7	3.83	5.66	1.48	1.53	1.43
8	2.42	4.64	1.92	1.88	1.84
Mean ± SD	2.86 ± 0.84	5.00 ± 0.57	1.80 ± 0.29	1.55 ± 0.32	1.54 ± 0.26

with MRTM2 ($r = 0.97$) than with MRTM ($r = 0.93$) and SRTM ($r = 0.93$). The slope of the line correlating BP from MRTM2 and 2-TCM was 0.82, while that from SRTM and 2-TCM was 0.75. This indicated that values from MRTM2 were 18% lower than those from 2-TCM (Fig. 7), although its degree of underestimation was smaller than that of SRTM (25%).

Effects of noise and start time on reference tissue analysis

To examine the cause of the 18% underestimation with MRTM2, we generated noise-free time–activity data and assessed in a stepwise manner the effects of t^* and noise itself. Noise-free dynamic brain concentrations of all measured regions were generated from preset (or "true") k values derived from 2-TCM and a measured input function in four monkeys with arterial blood sampling. With $t^* = 30$ min, the underestimation was reduced from 18 to 12% when comparing the real data to the noise-free data. When t^* was increased from 30 to 50 min with the noise-free data, the error was further reduced from 12 to 6% (Fig. 8A). This finding indicates that underestimation of BP in MRTM2 was derived from the noise and the early t^*. The degree of the underestimation was not changed in SRTM when comparing the real data to the noise-free data (25% with the real data and 26% with the noise-free data).

Although the majority of the scans lasted 90 min, three animals (Table I, Study 5 with Advance scanner and Studies 7 and 8 with HRRT scanner) had scans of 120 min. For these longer scans, we could delay t^* and still have adequate number of data points to estimate BP with linear reference tissue analysis. Within each data set, we compared BP calculated with t^* of 30 min using the initial 90 min of the scan with t^* of 50 min and the entire 120 min data. BP calculated with MRTM2 increased ~10% with the later start time and the longer duration scan (Fig. 8B). When we removed the data from Advance scanner under the consideration of the bias from using of different scanner, the similar degree of BP increase was shown (~14%). These results show that multilinear reference tissue analysis of [^{11}C](R)-(−)-RWAY monkey data can provide BP estimates very close to those of compartmental modeling, but they are prone to error in the presence of noise, an early start time, and a short scan duration.

Effect of P-gp on brain uptake and peripheral disposition of [^{11}C](R)-(−)-RWAY

Tariquidar (8 mg/kg i.v.) significantly increased the uptake of [^{11}C](R)-(−)-RWAY in all brain regions (Fig. 9A). In contrast, tariquidar had no significant effect on the clearance of [^{11}C](R)-(−)-RWAY measured in arterial plasma and corrected for radiometabolites (Fig. 9B). Tariquidar caused a ~55% increase of AUC (calculated from 0 to 90 min) in both target and background regions of brain (Table V). These results seemed to show a clear effect of P-gp blockade, i.e., increased brain uptake in the absence of noticeable changes of total tracer concentration in plasma. However, we also examined the effect of tariquidar on the free fraction (f_1) of tracer in plasma. Tariquidar increased f_1 in each animal, with a mean increase of (80 ± 29)% (Table V). The increased value of f_1 could more than fully explain the increased brain uptake caused by tariquidar. Thus, we have no evidence to conclude that [^{11}C](R)-(−)-RWAY is a substrate for P-gp in monkey brain.

DISCUSSION

The kinetics and distribution of brain uptake of [^{11}C](R)-(−)-RWAY are consistent with labeling of 5-HT$_{1A}$ receptors. Regions with low or negligible densities of receptors (e.g., cerebellum) showed rapid washout, and regions with high receptor densities (e.g., neocortex, dorsal raphe, and medial temporal region) maintained high levels of activities during latter portions of the scan. Furthermore, the uptake demonstrated stereoselectivity, since the uptake of the other enantiomer [^{11}C](S)-(+)-RWAY was similar to the cerebellar uptake of [^{11}C](R)-(−)-RWAY. Finally, brain uptake of [^{11}C](R)-(−)-RWAY could be displaced by WAY-100635, demonstrating that specific binding was selective for saturable 5-HT$_{1A}$ receptors. Thus, [^{11}C](R)-(−)-RWAY labels 5-HT$_{1A}$ receptors, but is it superior to [carbonyl-^{11}C]WAY-100635, which is currently the most popularly used radioligand for this target?

First, the synthesis of [^{11}C](R)-(−)-RWAY via O-^{11}C-methylation is significantly easier than the preparation of [carbonyl-^{11}C]WAY-100635. Second, the cerebellar uptake of [^{11}C](R)-(−)-RWAY in monkey is appro-

ximately five-fold greater than that of [carbonyl-^{11}C]WAY-100635 in human (Yasuno et al., 2004). Third, the amide bond of $[^{11}C](R)$-$(-)$-RWAY is reversed relative to that of WAY-100635 and is less vulnerable to metabolic hydrolysis at least in rodents (Shetty et al., 2005) and monkey (unpublished data). This study does not provide direct data to compare the clearance and metabolism of RWAY and WAY-100635. Nevertheless, metabolite fraction of $[^{11}C](R)$-$(-)$-RWAY in our data seems to be less than that of [carbonyl-^{11}C]WAY-100635 shown in the previous study (Gunn et al., 1998), and the clearance of $[^{11}C](R)$-$(-)$-RWAY in monkey is adequately fast to generate peak brain uptake within 20 min, which is an excellent time for ^{11}C that has a half-life of 20 min. Furthermore, we do not think that $[^{11}C](R)$-$(-)$-RWAY generates a similarly confounding radiometabolite in monkey, since estimates of V_T in cerebellum achieved 90% of target values by 60 min and increased by only 2–3% from 80 to 120 min (Fig. 6). So far, $[^{11}C](R)$-$(-)$-RWAY appears to be an excellent radiotracer for 5-HT$_{1A}$ receptors.

Effect of P-gp inhibition

To assess the potential effects of P-gp on $[^{11}C](R)$-$(-)$-RWAY, we used tariquidar, which is a potent inhibitor of P-gp (Roe et al., 1999). Tariquidar (8 mg/kg i.v.) increased brain uptake in target and reference regions of brain by ~50%, with insignificant change in the AUC of the parent tracer in plasma from 0 to 90 min (i.e., the amount of tracer exposed to brain). However, tariquidar increased f_1 by ~80%, which was more than adequate to account for the increased brain uptake. The effect on f_1 was a coincidental finding in a single study, which we then replicated in three separate experiments. We do not know why tariquidar increased f_1, but it may have simply displaced binding of $[^{11}C](R)$-$(-)$-RWAY to plasma proteins.

Was tariquidar administered at a dose sufficient to block P-gp at the blood–brain barrier? Previous studies have shown effective blockade at doses of 2.5–4.0 mg/kg i.v. and p.o. in rodents (Mistry et al., 2001) and 2 mg/kg i.v. in monkey (Talbot et al., 2003). In the light of the effect of tariquidar on f_1 and assuming that an adequate dose was administered, we have no evidence that $[^{11}C](R)$-$(-)$-RWAY is a substrate for P-gp in monkey.

Higher values of f_1 will make more drug available to diffuse through membrane barriers and thereby increase drug concentrations in the tissue. Displacement of a drug from plasma proteins and a corresponding increase in f_1 has frequently been associated with greater effects and toxicity of the medication (Susula and Atkinson, 2000). However, the effect is often transient, since the metabolism of the drug may also be increased. Since the PET scans last only 2 h, we would expect to see only the transient effects of increased concentration of free tracer in plasma, without coun-

terbalancing changes in tracer metabolism. Nevertheless, our results with P-gp blockade should be interpreted with caution because of the decreasing concentration of tariquidar that presumably occurs during the course of the scan. The values of f_1 are relatively low and difficult to measure with accuracy. The question of whether $[^{11}C](R)$-$(-)$-RWAY is a substrate of P-gp might better be examined with a P-gp blocker that does not interfere with radiotracer binding to plasma proteins.

Optimal analysis: compartmental versus reference tissue methods

Compartmental method

Fitting by 2-TCM was significantly better than by 1-TCM in all regions and all animals. A target region would be expected to have two-tissue compartments (i.e., nondisplaceable and receptor bound). The background region (i.e., cerebellum) would theoretically be expected to have only one-tissue compartment (i.e., nondisplaceable). Nevertheless, 2-TCM fits are often better than 1-TCM for background regions. Possible explanations for 2-TCM fitting of background regions include: (1) a radiometabolite that passes the blood–brain barrier (Gunn et al., 1998; Hall et al., 1997), (2) kinetically distinguishable nonspecific binding (Farde et al., 1998; Hall et al., 1997), and (3) tissue heterogeneity (Oikonen et al., 2000). Thus, the superior 2-TCM fit of cerebellar $[^{11}C](R)$-$(-)$-RWAY activity occurs with many radioligands and should not be used to disqualify the validity of compartmental fitting of this radioligand.

MRTM2 versus 2-TCM

MRTM2 has potential advantage over SRTM, in which the linearized models can be applied without assumption of a specific compartment configuration, as opposed to SRTM that assumes a 1T model for both the reference and target tissue regions (Lammerstma et al., 1996). Violations of this compartmental model assumption may be one of the cause of the biased BP estimates with SRTM in our data (Slifstein et al., 2000). In spite of this potential advantage, the slope of the correlation line indicated that BP values from MRTM2 were 18% lower than those from 2-TCM. The primary cause of this underestimation was that the scan duration of 90 min typically used for ^{11}C-labeled tracers was too short for the relatively slow kinetics of this ligand. The value of t^* should be selected as late as possible within the constraints of noise and scan duration, and BP will asymptotically approach true equilibrium values (Ichise et al., 2002). However, as t^* is increased (e.g., from 30 to 50 min) in real (i.e., "noisy") data, the remaining time to the end of the study (90 min) is too short, and BP is underestimated and sensitive to noise.

Despite their underestimation, results from reference tissue models were strongly correlated with those from 2-TCM and could be used in clinical studies if the underestimation is equivalent between individuals. Alternatively, longer scan duration can provide more accurate measurements of BP, so long as the later PET data are not inordinately contaminated with noise. We found in a subset of three experiments that increasing the scan duration from 90 to 120 min and t^* from 30 to 50 min, respectively, gave reference tissue measures of BP that were equivalent to 2-TCM. This comparison is valid only for the parameters of the current study, including injected activities of ∼220 MBq in anesthetized animals with negligible movement. Quantitation of [^{11}C](R)-(−)-RWAY with reference tissue methods in live subjects (e.g., humans) should carefully examine the effects of noise, scan duration, and injected activity.

In conclusion, [^{11}C](R)-(−)-RWAY is a useful tracer to measure 5-HT$_{1A}$ receptors in monkey brain. It is easily labeled, reaches peak levels in brain within 20 min, and does not show appreciable amounts of radiometabolites in brain. Although tariquidar increased brain uptake, the mechanism was probably displacement of the radiotracer from plasma proteins and a corresponding increase in f_1. For compartmental analysis using an arterial input function, two-tissue compartments are superior to one-tissue for both target and background regions. The uptake could be quantified with both arterial input compartmental and reference tissue methods, although the latter are prone to underestimation if the scan duration is short. These promising results justify trials of [^{11}C](R)-(−)-RWAY in humans with further investigation of analytical techniques that must be adapted to any species differences in plasma clearance and brain uptake and washout rates.

ACKNOWLEDGMENTS

REFERENCES

Akaike H. 1974. A new look at the statistical model identification. IEEE Trans Automat Control AC19:716–723.

Aloyo VJ, Harvey JA, Kirifides AL. 1993. Chronic cocaine increases win 35428 binding in rabbit caudate. Soc Neurosci Abstr 19:1843.

Ambudkar SV, Kimchi-Sarfaty C, Sauna ZE, Gottesman MM. 2003. P-glycoprotein: From genomics to mechanism. Oncogene 22:7468–7485.

Bevington PR, Robinson DK. 2003. Data reduction and error analysis for the physical sciences. New York: McGraw-Hill.

Burger C, Mikolajczyk K, Grodzki M, Rudnicki P, Szabatin M, Buck A. 1998. JAVA tools quantitative post-processing of brain PET data. J Nucl Med 39(Suppl):277.

Carson R. 1986. Parameter estimation in positron emission tomography. In: Phelps M, Mazziotta J, Schelbert H, editors. Positron emission tomography and autoradiography: Principles and applications for the brain and heart. New York: Raven Press. p 347–390.

Cunningham V, Lammertsma A. 1995. Radioligand studies in brain: Kinetic analysis of PET data. Med Chem Res 5:79–96.

Elsinga PH, Hendrikse NH, Bart J, Vaalburg W, van Waarde A. 2004. PET Studies on P-glycoprotein function in the blood–brain barrier: How it affects uptake and binding of drugs within the CNS. Curr Pharm Des 10:1493–1503.

Farde L, Ito H, Swahn C, Pike V, Halldin C. 1998. Quantitative analyses of carbonyl-carbon-11-WAY-100635 binding to central 5-hydroxytryptamine-1A receptors in man. J Nucl Med 39:1965–1971.

Gandelman MS, Baldwin RM, Zoghbi SS, Zea-Ponce Y, Innis RB. 1994. Evaluation of ultrafiltration for the free fraction determination of single photon emission computed tomography (SPECT) tracers: β-CIT, IBF, and iomazenil. J Pharm Sci 83:1014–1019.

Gunn RN, Sargent PA, Bench CJ, Rabiner EA, Osman S, Pike VW, Hume SP, Grasby PM, Lammertsma AA. 1998. Tracer kinetic modeling of the 5-HT$_{1A}$ receptor ligand [carbonyl-^{11}C]WAY-100635 for PET. Neuroimage 8:426–440.

Hall H, Lundkvist C, Halldin C, Farde L, Pike VW, McCarron JA, Fletcher A, Cliffe IA, Barf T, Wikström H, Sedvall G. 1997. Autoradiographic localization of 5-HT$_{1A}$ receptors in the post-mortem human brain using [^{3}H]WAY-100635 and [^{11}C]WAY-100635. Brain Res 745:96–108.

Hawkins RA, Phelps ME, Huang S-C. 1986. Effects of temporal sampling, glucose metabolic rates, and disruptions of the blood–brain barrier on the FDG model with and without a vascular compartment: Studies in human brain tumors with PET. J Cereb Blood Flow Metab 6:170–183.

Ichise M, Toyama H, Innis RB, Carson RE. 2002. Strategies to improve neuroreceptor parameter estimation by linear regression analysis. J Cereb Blood Flow Metab 22:1271–1281.

Ichise M, Liow JS, Lu JQ, Takano A, Model K, Toyama H, Suhara T, Suzuki K, Innis RB, Carson RE. 2003. Linearized reference tissue parametric imaging methods: Application to [^{11}C]DASB positron emission tomography studies of the serotonin transporter in human brain. J Cereb Blood Flow Metab 23:1096–1112.

Lammertsma AA, Hume SP. 1996. Simplified reference tissue model for PET receptor studies. Neuroimage 4:153–158.

Lammerstma AA, Bench CJ, Hume SP, Osman S, Gunn K, Brooks DJ, Frackowiak RS. 1996. Comparison of methods for analysis of clinical [11C]raclopride studies. J Cereb Blood Flow Metab 16:42–52.

Logan J, Fowler J, Volkow N, Wolf A, Dewey S, Schlyer D, MacGregor R, Hitzemann R, Bendriem B, Gatley S, Christman D. 1990. Graphical analysis of reversible radioligand binding from time-activity measurements applied to [N-^{11}C-methyl]-(−)cocaine PET studies in human subjects. J Cereb Blood Flow Metab 10:740–747.

McCarron JA, Turton DR, Pike VW, Poole KG. 1996. Remotely-controlled production of the 5-HT$_{1A}$ receptor radioligand, [carbonyl-^{11}C]WAY-100635 via ^{11}C-carboxylation of an immobilized Grignard reagent. J Labelled Compd Radiopharm 38:941–953.

McCarron JA, Chin F, Pike V, Hong J, Musachio J, Ichise M, Zoghbi S, Vines D, Vermeulen E, Wilstrom H, Halldin C, Innis R. 2004. New candidate PET radioligands for brain 5-HT$_{1A}$ receptors based on 2,3,4,5,6,7-hexahydro-1{4-[1[4-7(2-methoxyphenyl)-piperazinyl]]-2-phenylbutyryl}-1H-azepine (RWAY). Neuroimage 22(Suppl 2):T34–T35.

Mistry P, Stewart AJ, Dangerfield W, Okiji S, Liddle C, Bootle D, Plumb JA, Templeton D, Charlton P. 2001. In vitro and in vivo reversal of P-glycoprotein-mediated multidrug resistance by a novel potent modulator, XR9576. Cancer Res 61:749–758.

Oikonen V, Allonen T, Nagren K, Kajander J, Hietala J. 2000. Quantification of [carbonyl-^{11}C]WAY-100635 binding: Considerations on the cerebellum. Nucl Med Biol 27:483–486.

Osman S, Lundkvist C, Pike V, Halldin C, McCarron J, Swahn C-G, Farde L, Ginovart N, Luthra S, Gunn R, Bench C, Sargent P, Grasby P. 1998. Characterisation of the appearance of radioactive metabolites in monkey and human plasma from the 5-HT$_{1A}$ receptor radioligand [carbonyl-^{11}C]WAY-100635: Explanation of high signal contrast in PET and aid to biomathematical modeling. Nucl Med Biol 25:215–223.

Passchier J, van Waarde A, Doze P, Elsinga P, Vaalburg W. 2000. Influence of P-glycoprotein on brain uptake of [^{18}F]MPPF in rats. Eur J Pharmacol 407:273–280.

Paxinos G, Huang X-F, Toga A. 2000. The rhesus monkey brain in stereotaxic coordinates. San Diego: Academic Press.

Pike VW, McCarron JA, Hume SP, Ashworth S, Opacka-Juffry J, Osman S, Lammerstma AA, Poole KG, Fletcher A, White AC, Cliffe IA. 1995. Preclinical development of radioligand for studies of central 5-HT$_{1A}$ receptors in vivo-[^{11}C]WAY-100635. Med Chem Res 5:208.

Pike VW, McCarron JA, Lammerstma AA, Osman S, Hume SP, Sargent PA, Bench CJ, Cliffe IA, Fletcher A, Grasby PM. 1996.

Exquisite delineation of 5-HT$_{1A}$ receptors in human brain with PET and [carbonyl-^{11}C]WAY-100635. Eur J Pharmacol 301:R5–R7.

Roe M, Folkes A, Ashworth P, Brumwell J, Chima L, Hunjan S, Pretswell I, Dangerfield W, Ryder H, Charlton P. 1999. Reversal of P-glycoprotein mediated multidrug resistance by novel anthranilamide derivatives. Bioorg Med Chem Lett 9:595–600.

Shetty H, Zoghbi S, McCarron J, Liow J-S, Hong J, Pike V. 2005. Characterization of in vivo rat metabolites of [O-methyl-^{11}C]RWAY by LC-MS. J Labelled Compd Radiopharm 48(Suppl 1):278.

Slifstein M, Parsey R, Laruelle M. 2000. Derivation of [^{11}C]WAY-100635 binding parameters with reference tissue models: Effect of violations of model assumptions. Nucl Med Biol 27:487–492.

Susula GM, Atkinson JR. 2000.Effects of liver disease on pharmacokinetics. In: Atkinson JR, Daniels CE, Dedrick RL, Grudzinskas CV, Markey SP, editors. Principles of clinical pharmacology. San Diego: Academic Press. p 63–74.

Talbot P, Narendran R, Hwang D, Martinez D, Hackett E, Quadri N, Wood A, Wood M, Gorman J, Huang Y, Laruelle M. 2003. Modulation of brain delivery of the çopiate receptor agonist loperamide by P-glycoprotein inhibition: A PET study using [^{11}C]carfentanil in the baboon. J Nucl Med 44(Suppl):35.

Vaalburg W, Hendrikse N, Elsinga P, Bart J, van Waarde A. 2005. P-glycoprotein activity and biological response. Toxicol Appl Pharmacol 207:257–260.

Yasuno F, Suhara T, Ichimiya T, Takano A, Ando T, Okubo Y. 2004. Decreased 5-HT$_{1A}$ receptor binding in amygdala of schizophrenia. Biol Psychiatry 55:439–444.

Zoghbi SS, Shetty HU, Ichise M, Fujita M, Imaizumi M, Liow J-S, Shah J, Musachio JL, Pike VW, Innis RB. 2005. PET imaging of the dopamine transporter with [^{18}F]FECNT: A polar radiolabeled metabolite confounds brain radioligand measurements. J Nucl Med 47:520–527.